EUV high resolution imager on-board Solar Orbiter: optical design and detector performances

J.-P. Halain, A. Mazzoli, P. Rochus, E. Renotte, Y. Stockman
Centre Spatial de Liège
University of Liège
Angleur, Belgium
jphalain@ulg.ac.be

D. Berghmans, A. BenMoussa
Royal Observatory of Belgium
Brussels, Belgium

F. Auchère
Institut d'Astrophysique Spatiale
Orsay, France

***Abstract*— The EUV high resolution imager (HRI) channel of the Extreme Ultraviolet Imager (EUI) on-board Solar Orbiter will observe the solar atmospheric layers at 17.4 nm wavelength with a 200 km resolution.**

The HRI channel is based on a compact two mirrors off-axis design. The spectral selection is obtained by a multilayer coating deposited on the mirrors and by redundant Aluminum filters rejecting the visible and infrared light. The detector is a 2k x 2k array back-thinned silicon CMOS-APS with 10 µm pixel pitch, sensitive in the EUV wavelength range.

Due to the instrument compactness and the constraints on the optical design, the channel performance is very sensitive to the manufacturing, alignments and settling errors. A trade-off between two optical layouts was therefore performed to select the final optical design and to improve the mirror mounts. The effect of diffraction by the filter mesh support and by the mirror diffusion has been included in the overall error budget. Manufacturing of mirror and mounts has started and will result in thermo-mechanical validation on the EUI instrument structural and thermal model (STM).

Because of the limited channel entrance aperture and consequently the low input flux, the channel performance also relies on the detector EUV sensitivity, readout noise and dynamic range. Based on the characterization of a CMOS-APS back-side detector prototype, showing promising results, the EUI detector has been specified and is under development. These detectors will undergo a qualification program before being tested and integrated on the EUI instrument.

***Index Terms* — Extreme Ultraviolet, high-resolution imager, Solar Orbiter, CMOS-APS, Off-axis.**

I. Introduction

The Extreme Ultraviolet Imager (EUI) instrument on-board Solar Orbiter [1] is a three channels imager of the solar corona. It is composed of two high-resolution imager (HRI) and one full-sun imager (FSI). The two HRI will provide observation at the hydrogen Lyman-α line (HRI_{Lya}) [7] and in the extreme ultra-violet at 174 Å (HRI_{EUV}). The FSI is a dual band channel working alternatively at the two 174 Å and 304 Å passbands [2][3].

Fig. 1 shows the EUI optical unit with the main components of the three channels.

The spectral selection is obtained by multilayer coating deposited on the mirrors and by a set of transmission filters rejecting the visible and infrared light.

The detectors are 2k x 2k array for the HRI and a 3k x 3k array for the FSI channel. Back-thinned silicon CMOS-APS with 10 µm pixel pitch, sensitive in the EUV wavelength range are considered for the FSI and the HRI_{EUV} channels. A front side illuminated CMOS-APS is considered for the HRI_{Lya} channel.

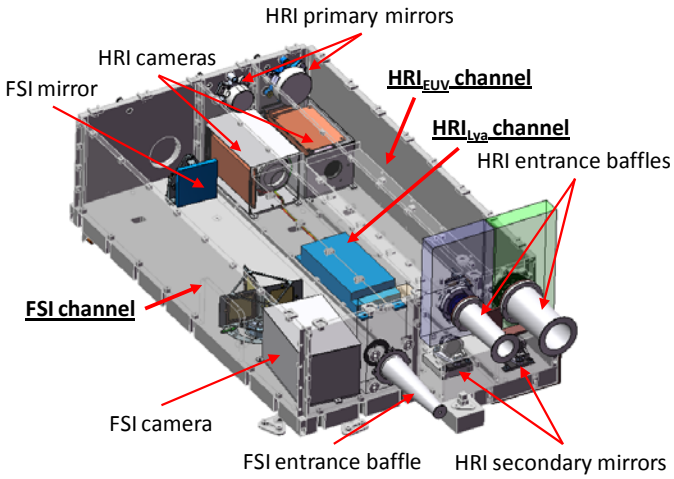

Fig. 1. EUI optical bench configuration

II. HRI_{EUV} Optical Design

A. Requirements

The driving requirements for the HRI_{EUV} channel optical design is summarized in TABLE I.

TABLE I. HRI_{EUV} CHANNEL REQUIREMENTS

Parameter	Requirement
Field of view	1000 arcsec square
Entrance pupil	47.4 mm diameter
Detector size	2048 x 2048 pixels 10 µm pixel pitch
Spot size	1 arcsec (i.e. 2 pixels)
Incident angles on mirrors	< 6 arcdeg
Spectral range	174 Å
Dimensions	< 820 mm length < 120 mm width

B. Design trade-off

A trade-off between an off-axis two mirrors Cassegrain or Gregory optical layout was performed with the objective of minimizing the spot size, taking into account the tolerancing error from manufacturing and alignment.

The Gregory has the advantage of an intermediate focus, allowing a fine baffling of the beam, but its spot size is by design larger than in the Cassegrain scheme. A Cassegrain optical design was therefore selected (layout is shown on Fig. 2, and parameters are given in Table II).

The entrance pupil is located at the entrance of a front baffle [5]. Two aluminum filters are used to reject infrared and visible light. One is placed at the end of the front baffle and the second one between the secondary mirror and the detector array [6].

The nominal Root Mean Square (RMS) spot diameter is always into the pixel size (10 µm) as shown in Fig. 3, between 0.7 and 4.3 µm. The design being diffraction limited into the 0 – 500 arcsec square range, the spot diameter (at 174 Å) only increases by 0.53 µm.

The design presents a very small distortion, lower than 0.1%. However, due to the off-axis design, the distortion is not symmetric.

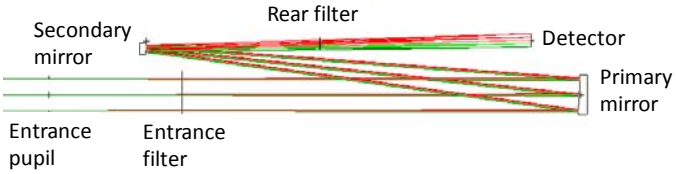

Fig. 2. EUI optical bench configuration

TABLE II. HRI_{EUV} CHANNEL CHARACTERISTICS

Focal length	4187 mm
Primary mirror	66 mm diameter (54 mm useful diameter) 80 mm off-axis R = 1518.067 mm CC K = -1
Secondary mirror	25 mm diameter (12 mm useful diameter) 11.44 mm off-axis R = 256.774 mm CC K = -2.0401375

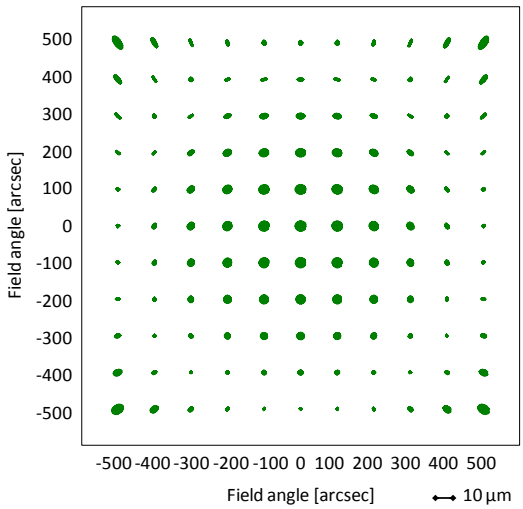

Fig. 3. HRI_{EUV} RMS spot size in the field of view

The angles of incidence on the primary and secondary mirrors are < 3.97 arcdeg and < 5.12 arcdeg respectively.

C. Figuring error

A figuring error onto both mirrors induces aberrations and a degradation of the optical performances.

Assuming a 3 nm RMS figuring error onto both mirrors (modelled by a mix of spherical aberration and astigmatism), it is shown that the design is very sensitive to this parameter. The optical performances are degraded up to 14 µm in diameter.

Fig. 4 gives the histograms of the degradation of the RMS spot diameter respectively at the centre and in a corner of the FOV (based on a statistical Monte Carlo analysis with a set of 500 samples).

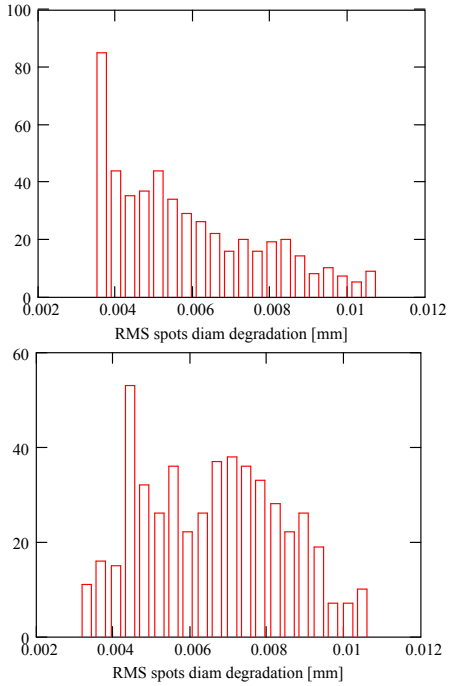

Fig. 4. Histograms of RMS spot diameter degradation at the centre and in corner of the field of view

D. Tolerancing

The tolerances are separated in three categories:

- The manufacturing tolerances contain the mirrors surface defects, the off-axis error and the roll error. The mirrors surface defects are represented by Zernike aberrations centred on the useful aperture. They are separated in focus, cylinder and the other aberrations. The cylinder contains focus, astigmatism and coma. The other aberrations contain the 32 first Zernike terms except focus, astigmatism and coma.
- The alignment tolerances contain the errors in position and orientation of the mirrors.
- The setting tolerances contain the accuracy on position and orientation of the mirrors used as compensator. There is no setting on the position of the primary (only secondary orientation is used for the compensation).

TABLE III presents the results of the degradation of RMS spots size at 3 sigma for each tolerance type (Monte Carlo analysis). The last row gives the RMS spots considering the root mean square sum of the nominal spot size with the arithmetic sum of the three tolerance contributions.

TABLE III. HRI_{EUV} CHANNEL TOLERANCING (SPOT SIZE IN µM VERSUS POSITION IN THE FIELD OF VIEW IN ARCSEC)

	0 0	**0 250**	**250 -250**	**250 0**	**0 500**	**0 -500**	**-500 0**	**-500 -500**
Nominal	3.7	2.8	1.9	2.8	1.1	0.4	0.7	4.3
Manufact.	6.8	7.1	7.8	7.1	8.7	9.4	8.9	8.5
Alignment	0.5	0.1	0.3	0.6	0.2	0.3	0.5	0.1
Settings	2.8	2.1	3.6	3.3	1.4	1.2	0.5	2.6
TOTAL	10.8	9.7	11.8	11.3	10.4	10.9	9.9	12.0

The final size of the image spots will have 99 % of chance to be below 12 µm (at 3 sigma). This spot size is close to the pixel size (10 µm) and ensures that the energy stays in two pixels as required (TABLE II).

Fig. 4 shows the errors budget considering the tolerancing, the thermal contribution, the settlings and the mirrors scattering (value to be computed). The filter diffraction and mirrors diffusion scattering are included in the error budget for clarity, but only add a lower intensity value ('wings') around the point spread function (PSF) which shall not be considered for the total width of this PSF.

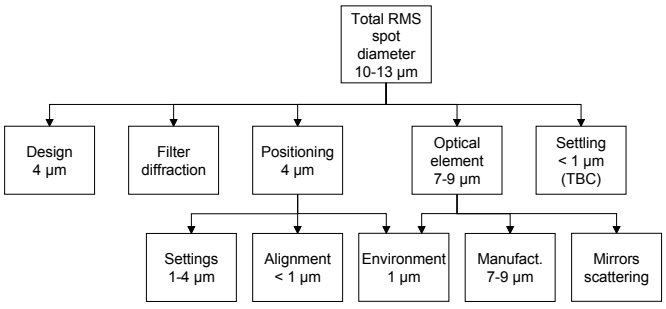

Fig. 5. Errors budget on the HRI_{EUV} RMS spot size

III. DETECTOR PERFORMANCES

A. Detector needs

Because of the limited channel entrance aperture (47.4 mm diameter) and consequently the low input flux (< 20 ph/px/s on the detector for coronal holes, < 100 ph/px/s for quite Sun and < 900 ph/px/s for active regions), the channel performance relies on the detector EUV sensitivity, readout noise and dynamic range.

The EUI telescopes will use large-format (2k x 2K for the HRI channels and 3k x 3k for the FSI channel) CMOS radiation-hardened active-pixel image sensor (APS) allowing shutterless operation. For the EUV channels, backside illuminated, thinned APS, sensitive in the EUV is considered. For the Ly-α channel, a front side illuminated, sensitive in the visible (VIS), will be used with an intensifier [7]. In addition, a great radiation tolerance is required because of the harsh environment of the Solar Orbiter mission, in order to limit charge transfer. Low power consumption and an operational temperature at -40 °C are design constraints.

B. Detector prototypes

A back and a front side version of an APS detector prototype have been developed on the basis of the EUI specifications, and were characterized as part of the preliminary development phase of the instrument. The EUI detector prototypes were named APSOLUTE for APS Optimized for Low-noise and Ultraviolet Tests and Experiments.

Two APSOLUTE image sensors were designed (Fig. 6) and procured by the Belgian CMOSIS company:

- A 256 x 256 pixel array, containing 16 test pixel variants, organized in blocks of 64 x 64 pixels to select the best pixel design variant to be used in later flight devices.
- A 1024 x 1024 pixel array, containing the best guess pixel variant out of the 16 variants. Its size is close to the flight model size to validate manufacturing process (in particular back thinning) and large-scale performances.

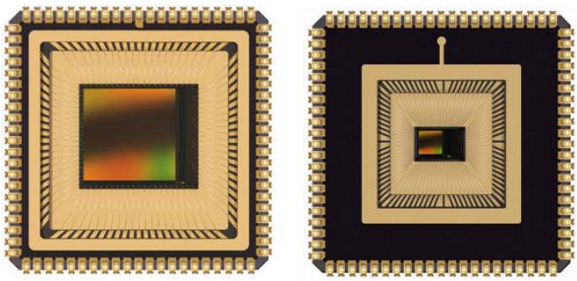

Fig. 6. APS prototypes developed to validate the EUI detector baseline

To achieve the requested high dynamic range, two gain paths are available per pixel. This results in 2 x N outputs per line of N pixels. 2 x N column gain stages are implemented. Each column multiplexer sends 2 x N data to a single analog output channel. The output stage converts the signal to a fully-

differential signal which can be sent to an off-chip A/D converter. An Serial Peripheral Interface (SPI) is used to control various sensor settings (bias currents, voltage levels, gains…) and a temperature sensor is read out over the SPI interface.

The prototype detectors tests included flat field and MTF measurement, dark current characterization versus temperature, photon transfer curve (PTC) characterization (Fig. 7), EUV response (Fig. 8). These tests were performed before and after radiation hardness tests, i.e. Total Ionizing Dose (TID), Heavy Ions (HI) and Protons irradiation.

The complete sequence demonstrated the suitability of the CMOS-APS technology as the baseline detector and reaching the required qualification status (i.e. a radiation tolerant APS detector with very low noise, large dynamic range and EUV sensitivity).

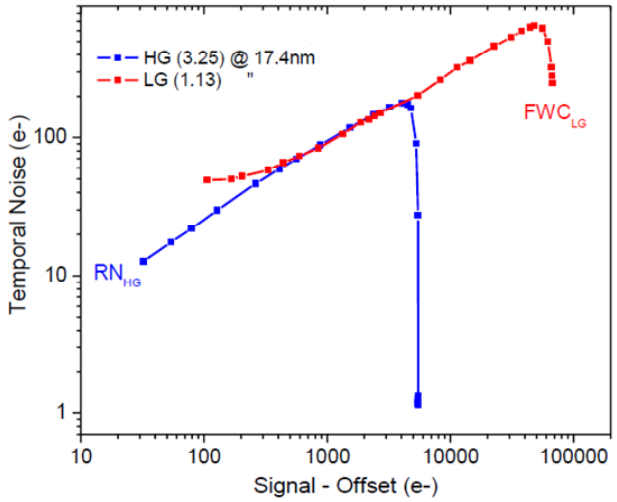

Fig. 7. PTC measured at 17.4 nm, for high and low gains, on a 1k x 1k back-side prototype

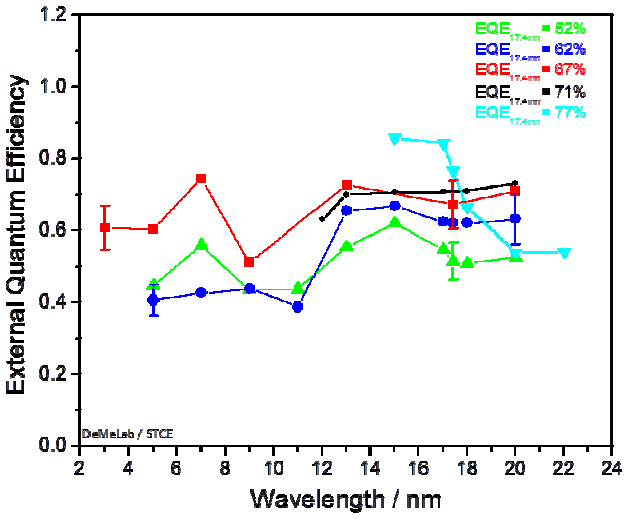

Fig. 8. Measured detector response in the EUV wavelengths of EUI APS detector prototypes

TABLE IV summarizes the detector prototype test results, as compared with EUI detector requirements.

TABLE IV. PROTOTYPE TEST RESULTS AS COMPARED WITH EUI DETECTOR REQUIREMENTS

Parameter	Flight Requirement	Prototype results
Number of pixels	2k x 2k (HRI) 3k x 3k (FSI)	1k x 1k and 256 x 256
Pixel pitch	10 µm	10 µm
Spectral range	10-40 nm (EUV) 121 nm (Ly-a)	Measured 5 – 20 nm and 325 – 1025 nm.
Maximum pixel rate (frame rate)	10 FPS	10 FPS
MTF / optical crosstalk	50% / 5%	> 50% (in visible)
Sensitivity (detected ph/incident ph)	> 50%	> 50% at 17.4 nm
Readout noise	< 5 e^- RMS	< 4 e^- (on back-side devices)
Average dark signal	10 e^-/s/px	Achieved at -40 °C.
Pixel saturation charge	> 80 ke^-	Up to 83 ke^- at linear full well capacity (on back-side)
Non-linearity (p-p)	< 2 %	< 2%
Power consumption	< 0.5 W	~ 0.1 W
Radiation hardness	>30 kRad	>100 kRad (on back-side)
Operational T° range	-60 / +60 °C	Tested from -60 °C to +60 °C

IV. MANUFACTURING AND TEST

Manufacturing of the FSI mirror and mount has been initiated (Fig. 9). For the HRI channels, the mount detailed design has been performed taking into account the alignment needs and the mechanical constraints of the interfaces (Fig. 10).

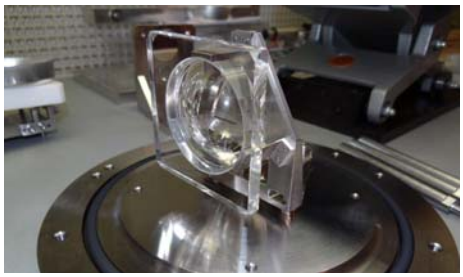

Fig. 9. First FSI mirror batch

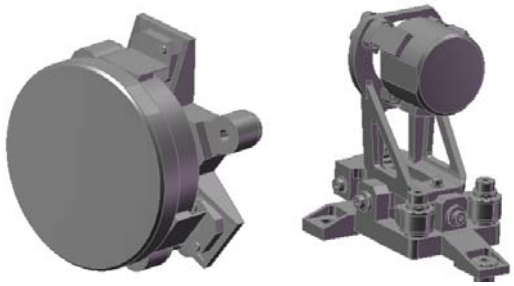

Fig. 10. HRI_{EUV} primary (left) and secondary (right) mirror and mirror mount detailed design.

Thermo-mechanical validation will be carried out on the EUI instrument structural and thermal model (STM) during the thermal balance test. The EUI OBS unit will be mounted in a thermal shroud and on a mechanism allowing to pitch the unit by +/- 10 arcdeg (to simulate thermal impact of off-pointing versus Sun simulator direction), as shown on Fig. 11.

One objective of the thermal balance test is to validate the stability of the HRI mirror mounts over the temperature operational range (-30 °C to +50 °C) by auto-collimation on flat dummy mirrors on flight representative mirror mounts. The unit alignment cube will also be used to validate the unit stability over the temperature range and to discriminate potential mirror tilt due to optical bench bending and or bench bipods torsion.

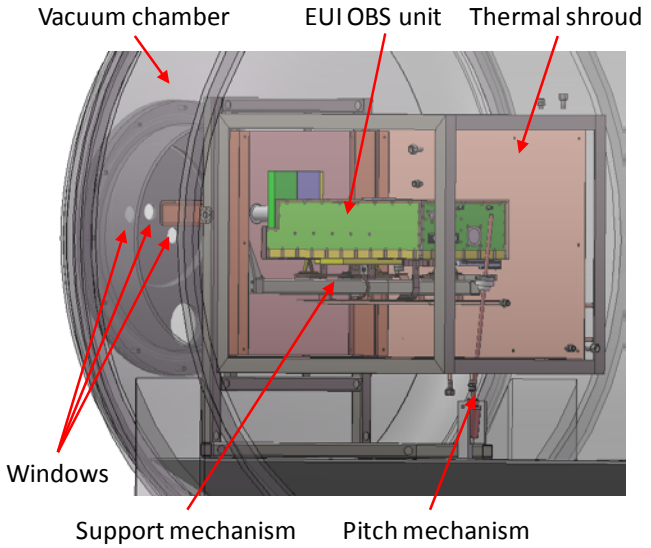

Fig. 11. Configuration for the EUI OBS unit STM thermal balance test.

Conclusions

The HRI_{EUV} channel of the EUI instrument is the most challenging in term of optical performance. A two-mirror Cassegrain optical layout has been selected to ensure the spot size is in the requirements when taking into account the manufacturing tolerances.

In term of sensitivity, the HRI_{EUV} channel is also critical and a dedicated APS detector has been designed. A set of detector prototypes were tested as part of the overall channel performance validation.

Next step is to perform thermo-elastic validation of the EUI instrument, and in particular of the HRI_{EUV} channel to validate the mirror mounts and the structure stability.

Acknowledgment

The EUI instrument is developed in a collaboration which includes the Centre Spatial de Liège and Royal Observatory of Belgium (Belgium), the Institut d'Astrophysique and Institut d'Optique (France), the UCL Mullard Space Science Laboratory (UK), the Max Planck Institute for Solar System Research (Germany) and the Physikalisch-Meteorologisches Observatorium Davos (Switzerland). The Belgian institutions are funded by the Belgian Federal Science Policy Office; the French institutions by the Centre National d'Etudes Spatiales (CNES), the UK institution by the UK Space Agency (UKSA), the German institution by Deutsche Zentrum für Luft- und Raumfahrt e.V. (DLR), and the Swiss institution by the Swiss Space Office (SSO).

References

[1] Marsden R.G., Marsch E. and the Solar Orbiter Science Definition Team, "Solar Orbiter Science Requirements Document", SCI-SH/2005/100/RGM Issue 1 Revision 2 (2005).

[2] Rochus P., Halain J.P., Renotte E., Berghmans D., Zhukov A., Hochedez J.F., Appourchaux T., Auchère F., Harra L.K, Schühle U., Mercier R.., "The Extreme Ultraviolet Imager (EUI) on-board the Solar orbiter Mission", 60th International Astronautical Congress (2009).

[3] Hochedez J.-F., Appourchaux T., Defise J.-M., Harra L. K., Schuehle U., Auchère F., Curdt W., Hancock B., Kretzschmar M., Lawrence G., Marsch E., Parenti S., Podladchikova E., Rochus P., Rodriguez L., Rouesnel F., Solanki S., Teriaca L., Van Driel L., Vial J.-C., Winter B., Zhukov A., "EUI, The Ultraviolet Imaging Telescopes of Solar Orbiter", The Second Solar Orbiter Workshop (2006).

[4] Auchère F., Ravet-Krill M.-F., Moses J.D., Rouesnel F., Moalic J.-P., Barbet D., Hecquet C., Jérome A., Mercier R.; Leclec'h J.-C., Delmotte F., Newmark J.S., "HECOR, a HElium CORonagraph aboard the Herschel sounding rocket", Proc. SPIE, 6689, 11 (2007).

[5] Halain J.-P., Rochus P., Appourchaux T., Berghmans D., Harra L., Schühle U., Auchère F., Zhukov A., Renotte E., Defise J.-M., Rossi L., Fleury-Frenette K., Jacques L., Hochedez J.-F., Ben Moussa A., "The technical challenges of the Solar-Orbiter EUI instrument", Proc. SPIE 7732, 26 (2010)

[6] Halain J.-P., Houbrechts Y., Auchère F., Rochus P., Appourchaux T., Berghmans D., Schühle U., Harra L., Renotte E., Zukhov A., The Solar-Orbiter EUI Instrument Optical Developments, ICSO (2010).

[7] Schühle, U., Halain, J., Meining, S., Teriaca, L., "The Lyman-alpha telescope of the extreme ultraviolet imager on Solar Orbiter" in Solar Physics and Space Weather Instrumentation IV, edited by Silvano Fineschi, Judy Fennelly, Proc. SPIE 8148 (2011)

[8] Halain, J.-P., Rochus P., Renotte E., Appourchaux T., Berghmans D., Harra, L., Schühle, U. , Schmutz, W., Auchère, F., Zhukov, A., Dumesnil, C., Delmotte, F., Kennedy, T., Mercier, R., Pfiffner, D., Rossi, L., Tandy, J., BenMoussa, A., Smith, P., "The EUI instrument on board the Solar Orbiter mission: from breadboard and prototypes to instrument model validation", Proc. SPIE 8443, 6 (2012).